



OPEN Cybersickness-induced EEG responses in curved monitor and head-mounted display

Dong-Hyun Lee^{1,2}, Kyoung-Mi Jang³ & Hyun Kyoon Lim^{1,2}✉

Cybersickness is a common issue in virtual reality (VR), yet addressing it remains challenging due to the lack of quantitative evaluation methods. To quantitatively assess cybersickness, this study examined electroencephalography (EEG) changes and Simulator Sickness Questionnaire (SSQ) scores using two different display types: a curved monitor and a head-mounted display (HMD). Thirty-one male participants (25.0 ± 1.9 years old) were exposed to cybersickness-inducing VR content developed using the Unity engine, featuring pitch, yaw, and roll rotations. The results revealed two key findings. First, regarding cybersickness induction, both display conditions showed significant increases in Delta power and decreases in Alpha power compared to the baseline, thus validating the effectiveness of the stimulus. Second, in the direct comparison between the two displays, no statistically significant differences were found in EEG spectral power. However, SSQ scores showed significantly higher Disorientation in the HMD condition. Furthermore, no linear correlation was observed between EEG and SSQ scores. In conclusion, these findings suggest that although both displays trigger similar physiological responses associated with sensory conflict processing (EEG), the immersive HMD environment induces greater vestibular disorientation (SSQ). This implies that a curved monitor may be a viable alternative for studying the physiological correlates of cybersickness.

Keywords Cybersickness, Virtual reality, Electroencephalography

In the early days of virtual reality (VR) technology, there was hope that it would be widely adopted across various fields¹. However, due to certain technical limitations, its application did not progress as initially anticipated¹. More recently, advancements in VR technology have made it increasingly viable for use in areas such as military training, education, and research, owing to its immersive and interactive nature². Improvements in display technologies, including desktop and head-mounted displays (HMDs), have also made it easier for users to experience 3D visual information³. Despite these advances, prolonged use of these displays can still result in discomfort a condition known as cybersickness⁴. Approximately 80% of participants who had prior experience with HMD-based VR reported feeling uncomfortable after just 10 min of exposure to the virtual environment⁵. This high prevalence highlights the importance of developing a quantitative assessment to address cybersickness.

The symptoms of cybersickness are similar to those of common motion sickness, including nausea, dizziness, and disorientation⁵. Several theories have been proposed to explain the cause of motion sickness, such as the evolutionary theory, postural instability theory, and sensory conflict theory, but the precise cause is not yet fully understood⁶. Among these, sensory conflict theory, which suggests that motion sickness arises from a conflict between the visual and vestibular systems, is widely accepted and cited⁷. Cybersickness has been referred to by various terms, including Visually Induced Motion Sickness (VIMS), VR sickness, and simulator sickness, in different studies⁸. In this study, we use the term cybersickness to include VIMS, VR sickness, and simulator sickness in different studies.

Subjective assessments typically use tools like the Simulator Sickness Questionnaire (SSQ), which rely on the participant's memory of rapidly changing symptoms, as they are usually administered only before and after VR use⁹. This dependence on memory makes it challenging to measure cybersickness quantitatively in real-time^{10–12}. On the other hand, objective methods assess cybersickness using biosignals, such as brain waves, heart rate, gastrointestinal reactions, and electrodermal (EDA) responses^{13–16}. Among these, EEG has recently been utilized to investigate cybersickness due to its high temporal and spatial resolution, which allows for real-time monitoring of changes in brain activity during VR experiences^{17,18}.

¹Division of Biomedical Metrology, Korea Research Institute of Standards and Science (KRISS), Daejeon 34113, Republic of Korea. ²Department of Precision Measurement Engineering, University of Science and Technology (UST), Daejeon 34113, Republic of Korea. ³Digital Health Research Division, Korea Institute of Oriental Medicine (KIOM), Daejeon 34054, Republic of Korea. ✉email: hlim@kriss.re.kr

The causes of cybersickness can generally be classified into content, human factors, and hardware^{2,19,20}. Particularly in terms of hardware, many studies have focused on display type, head tracking, field of view (FOV), latency, and other factors². Studies on cybersickness related to differences in display type have been conducted using various systems, including HMD and desktop monitor. These studies either used a single display or compared multiple display types. A study comparing HMD to flat monitor (televisions) under different viewing conditions, such as playing stereoscopic games or passively watching videos, used tools like the Simulator Sickness Questionnaire (SSQ) to assess cybersickness²¹. Others assessed cybersickness using subjective SSQ scores across four types of displays, including HMD, monitor, theater, and screen²². A comparison of flat monitor, stereoscopic monitor, and HMD explored the role of content depth in relation to different displays, emphasizing the importance of visual information in the perception of depth and distance²³. One study compared CAVE, HMD, and desktop monitor using EDA and several questionnaires to assess cybersickness²⁴. Cybersickness was also evaluated using both objective measures, including electrocardiography (ECG), EDA, postural sway, and photoplethysmography (PPG), and subjective ratings based on Bagshaw and Stott's scale in a study comparing HMD and desktop monitor²⁵. In a study where HMD and screen conditions were presented with identical visual stimuli, head immobilization using a chin rest was applied, and cybersickness was measured using the Fast Motion Sickness Scale (FMS) and a questionnaire²⁶. Many previous studies on display types have focused on comparing HMD with flat displays. However, recent advancements in hardware have introduced curved monitors, which have been suggested to enhance immersion^{27,28}. Curved monitors may provide this effect by engaging the user's peripheral vision and creating a stronger sense of depth, a goal that is also pursued by HMD. While both display types seek to increase immersion, they appear to rely on distinct mechanisms, which could differentially influence the onset of cybersickness. Therefore, a comparison between these two immersive display technologies may provide useful insights into their distinct mechanisms of immersion and their impacts on cybersickness onset.

In the present study, EEG was used to quantitatively assess and compare cybersickness based on EEG frequency and brain region across two display types (HMD and curved monitor), with participants viewing the same 3D image designed to induce cybersickness. A subjective assessment of cybersickness was also conducted using the SSQ.

Methods

Participants

Based on an a priori power analysis targeting a medium effect size (Cohen's $d = 0.5$; $\alpha = 0.05$; $1 - \beta$ (beta) = 0.80), which indicated a required sample size of 34, we initially recruited thirty-three males in their 20s. However, two participants withdrew due to severe cybersickness symptoms. Thirty-one males in their 20s (25.0 ± 1.9 years old) participated in this experiment. Participants were selected based on their susceptibility to motion sickness and assessed using the MSSQ (Motion Sickness Susceptibility Questionnaire to induce cybersickness). Out of the 858 participants who took the MSSQ test, 31 individuals exceeded the 75th percentile score (21.6) for 20-year-old males found in a prior study, achieving an average score of 31.0 ± 6.5 . Some studies have suggested that differences in cybersickness susceptibility may be influenced by factors such as hormones, field of view, and sensitivity to motion sickness^{29,30}. Accordingly, to minimize potential confounding effects, only male participants in their 20s, who were able to take part in the present experiment without difficulty, were selected. The study was approved by the ethics committees of the Korean Research Institute for Standards and Science (KRIS-IRB-2021-03 and KRIS-IRB-2022-03). All procedures were performed in accordance with the relevant guidelines and regulations, and the study was conducted in accordance with the Declaration of Helsinki. Written informed consent was obtained from all participants prior to their participation. All participants were in good health and were not taking any medications that could affect brain function or emotions.

Questionnaires

MSSQ assesses susceptibility to motion sickness based on nine different sources, including cars, buses, trains, airplanes, small boats, ships, and playground swings. It evaluates motion sickness experienced during childhood (before age 12, referred to as A) and in adulthood (over the past 10 years, referred to as B), using a frequency scale ranging from 0 (never experienced) to 3 (experienced very often).

SSQ measures cybersickness through 16 symptoms, each rated on a four-point scale from 0 to 3, with higher scores indicating more severe symptoms. The SSQ is divided into three factors: nausea, oculomotor, and disorientation. The experiment was conducted over a two-week period and included a pre-experiment SSQ (Pre-SSQ), three post-session SSQs (SSQ1, SSQ2 and SSQ3), and a post-recovery SSQ (Post-SSQ) after the participants had sufficiently recovered from cybersickness.

VR content

In this study, VR content was created using the Unity game engine (Unity Technologies) to induce cybersickness. The cybersickness-inducing video was viewed three times, with one viewing session per week over the course of two weeks. The content was displayed on a 49-inch curved monitor (3840×1080 pixels, 1195.8×336.3 mm) and via a HMD device (HTC Vive Pro). The HMD features a dual AMOLED display with a resolution of 1440×1600 pixels per eye, a refresh rate of 90 Hz, and a motion-to-photon latency of less than 20 ms. The headset weighs approximately 770 g. In this paper, we refer to curved-VR as viewing the content on the curved monitor and HMD-VR as viewing the content on the HMD. The VR content was 1 min long and consisted of 3 rotations (pitch, yaw, and roll), zoom in, and zoom out to induce cybersickness. The movement velocity was 8 m/s and the angular velocity was $60^\circ/\text{s}$, selected from a pilot study by the authors as the appropriate threshold to induce cybersickness. The motion was designed to be continuous rather than sudden to simulate a coherent visual flow. Although the trajectory was randomized during content generation to prevent prediction, the identical

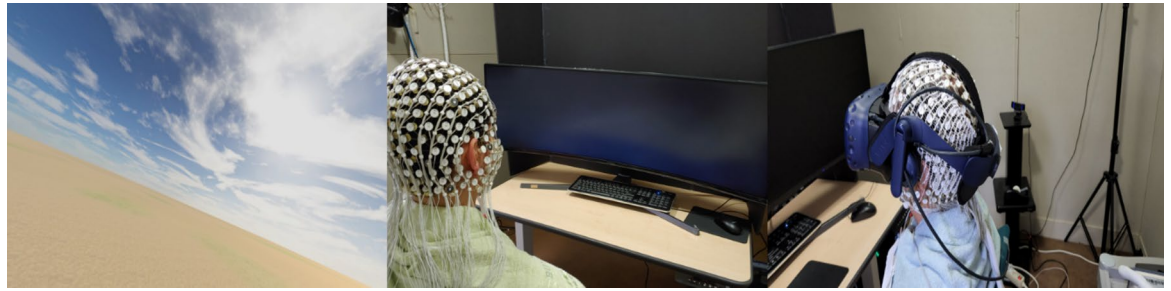


Fig. 1. From left to right: VR Content, curved-VR, and HMD-VR.

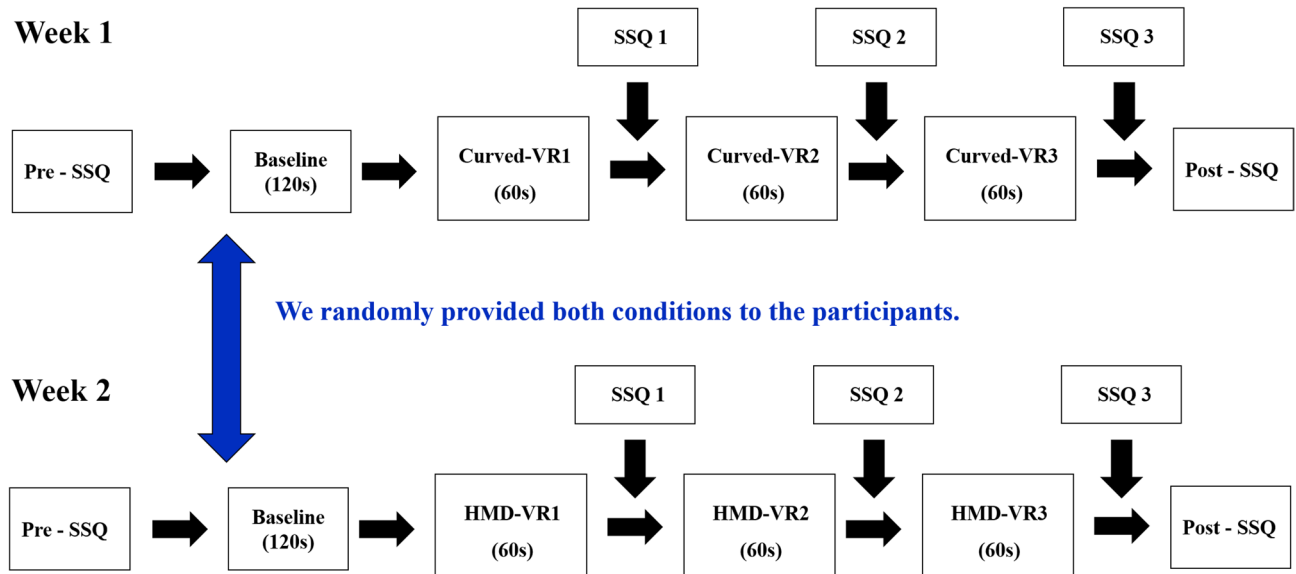


Fig. 2. Experimental protocol.

pre-rendered video sequence was applied across all participants and conditions to ensure strict experimental consistency. In this study, the Field of View (FOV) of a curved monitor and HMD were compared at a viewing distance of 65 cm for visual field comparison. The curved monitor was calculated to provide a horizontal FOV of approximately 85.5 degrees and a vertical FOV of 44.1 degrees. Additionally, in the HMD condition, head tracking was enabled to prevent sensory conflict. However, all participants were instructed to maintain a fixed head position in both conditions, ensuring that the visual stimulation remained comparable between the curved monitor and the HMD (Fig. 1).

Experimental protocol

Participants took part in the experiment on the same day of the week at the same time for a total of two weeks. They all completed a Pre-SSQ before the start of the experiment to determine whether or not they were susceptible to motion sickness, and then viewed the VR content using the curved monitor and the HMD device. To randomize the order of curved-VR and HMD-VR, we chose one display method for week 1 and the other for week 2. For curved-VR, participants were asked to rest motionless and open-eyed for 2 min for baseline, after which they were informed that the VR content would begin and asked to focus on the visual stimuli. Similarly, for HMD-VR, the baseline involved resting with the HMD on, eyes open, and body immobile, and after the baseline, participants were informed that the VR content would begin and instructed to focus on the visual stimuli. The VR content was repeated three times, with each viewing lasting 60 s (Fig. 2). Between viewings, participants were given a 5-minute break to recover from cybersickness and were asked to complete the SSQ verbally during the break. After the third viewing, participants were given enough time to fully recover, and completed the Post-SSQ once they felt recovered from motion sickness (Fig. 2).

EEG recording and data process

EEG measurements were made using a 256-channel HydroCel Geodesic Sensor (Net Amp 400; Electrical Geodesics Incorporated, Eugene, OR) with Cz as the reference electrode, keeping the impedance below 50 k Ω . EEG data were recorded using a 0.01–200 Hz bandpass filter at a sampling rate of 1000 Hz and preprocessed with a 1–50 Hz bandpass filter. To minimize noise from the HMD and other artifacts, channels with excessive noise

were visually inspected and removed, including a total of 73 channels located on the cheeks, neck, and outer scalp areas. The remaining 184 channels were then re-referenced to the average of all selected channels. Following re-referencing, the data were subjected to Independent Component Analysis (ICA) using the Matlab-based EEGLab toolbox to remove remaining artifacts such as eye movements, blinks, ECG, and electromyography (EMG). To minimize noise, a stable 20 s segment was extracted and analyzed from the 120 s baseline for a participants. In the VR content, the analysis focused on the final 20 s of the exposor. This specific time window was selected based on prior research indicating that cybersickness severity increases with exposure duration³¹. These continuous EEG data were down-sampled to 250 Hz and analyzed using Fast Fourier transform (FFT) to spectrally classify the absolute power of the EEG in five regions (frontal, central, parietal, occipital, and temporal): delta (1–4 Hz), theta (4–8 Hz), alpha (8–13 Hz), beta (13–30 Hz), and gamma (30–50 Hz). For the FFT analysis, the segments were set to a 2-s window with a 50% overlap. The absolute power in each region was calculated by averaging the power of the designated channels: frontal (average of 42 channels), central (average of 32 channels), parietal (average of 34 channels), occipital (average of 18 channels), and temporal (average of 20 channels) (Fig. 3).

Statistical analysis

All statistical analyses were performed using SPSS 29 software. For each participant, after conducting the experiment three times under both the curved-VR and HMD-VR conditions, EEG data from each condition were averaged to generate the mean value per condition. First, cybersickness induction was assessed by performing a paired t-test comparing baseline EEG with the average EEG during cybersickness induction. To compare the two VR conditions, for normalization, change scores were calculated by subtracting baseline EEG from the averaged EEG of each VR condition, and a paired t-test was then performed on these change scores. To verify the statistical robustness of these results, a supplementary Analysis of Covariance (ANCOVA) was conducted using the absolute EEG power, with baseline values included as covariates. This analysis aimed to confirm whether controlling for baseline variability altered the study outcomes. To control for the increased risk of Type I errors due to multiple comparisons across these 25 band-region combinations, Bonferroni correction was applied, setting the significance level to $p < 0.002$. Additionally, SSQ scores between the curved-VR and HMD-VR sessions were compared using a paired t-test, and Pearson correlations were calculated to assess their relationship with EEG.

Results

Evaluate cybersickness within each display

The delta waves in the frontal region significantly increased in curved-VR compared to baseline ($p < 0.05$). Theta waves also increased in the parietal region ($p < 0.05$), while alpha waves decreased from baseline in the frontal ($p < 0.05$), central ($p < 0.001$), parietal ($p < 0.01$), occipital ($p < 0.001$), and temporal ($p < 0.001$) regions. Beta waves showed an increase in the frontal region ($p < 0.001$) and a decrease in the parietal region ($p < 0.05$), while gamma waves increased in the frontal region ($p < 0.001$) and decreased in the central region ($p < 0.01$). Table 1 presents significant differences in the absolute power of all frequency bands across all regions between baseline and curved-VR. The topographical distribution of all frequency bands for baseline and curved-VR is shown in Fig. 4.

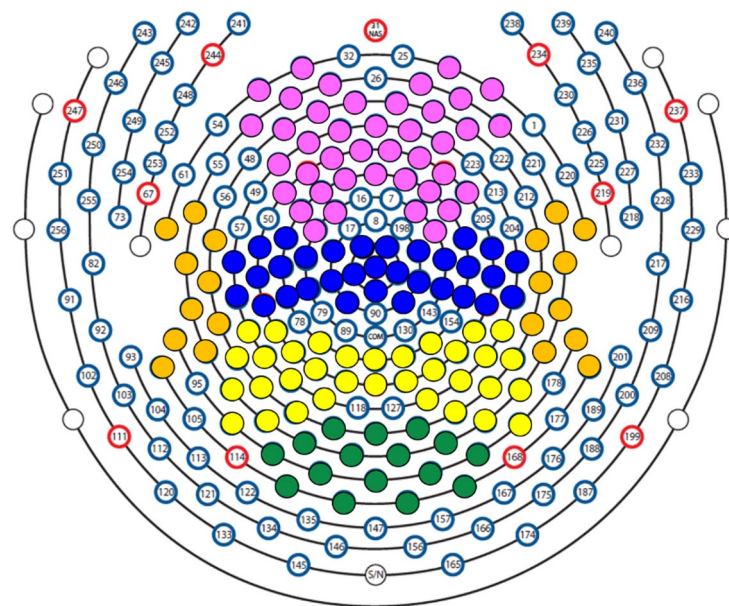


Fig. 3. Channel locations for EEG recording: Frontal (pink), Central (blue), Parietal (yellow), Occipital (green), and Temporal (orange) areas.

Curved-VR	Frontal	Central	Parietal	Occipital	Temporal
Delta	Up * (147%)	/	/	/	/
Theta	/	/	Up * (83%)	/	/
Alpha	Down * (63%)	Down *** (52%)	Down ** (41%)	Down *** (40%)	Down *** (59%)
Beta	Up *** (128%)	/	Down ** (82%)	/	/
Gamma	Up *** (140%)	Up * (113%)	/	/	/

Table 1. Significant changes in EEG frequency and area between baseline and induced cybersickness on a curved monitor ($n=31$).

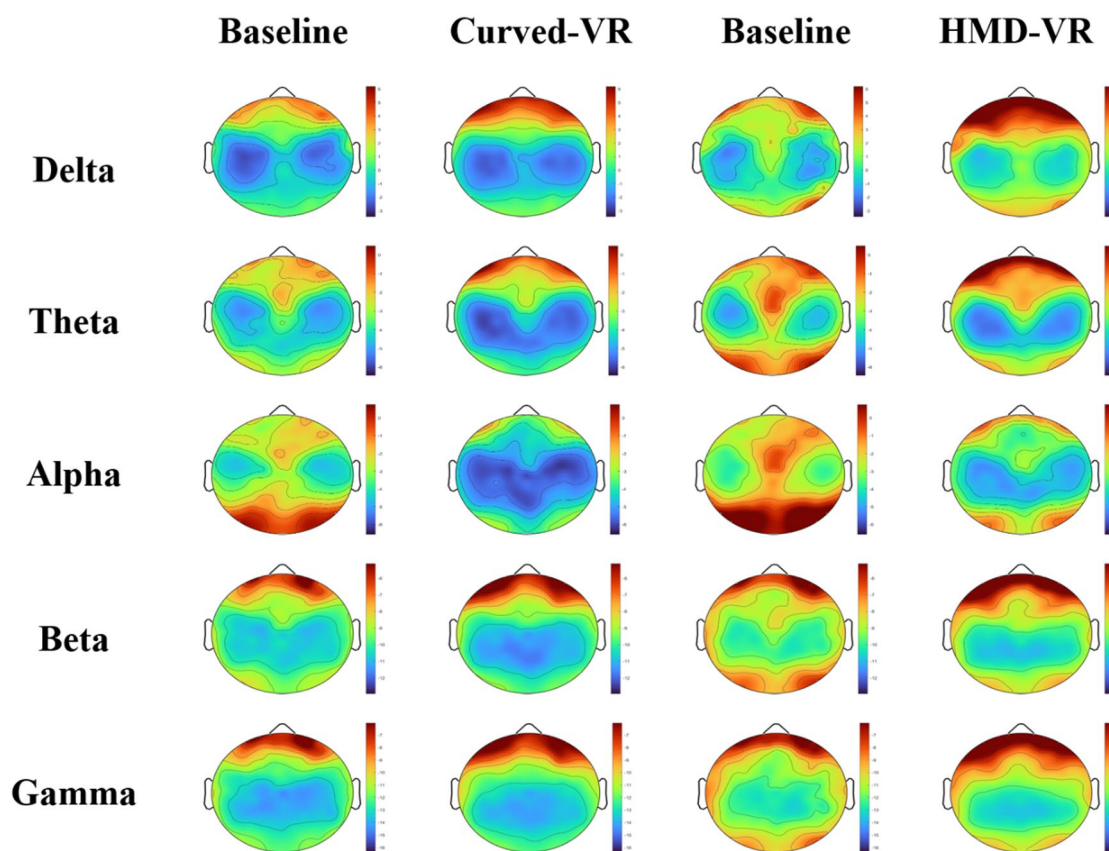


Fig. 4. Comparison of EEG power in each frequency band across baseline, curved-VR, and HMD-VR conditions.

Here “Up” indicates significantly increased EEG frequencies compared to the baseline and “Down” means the opposite. The (n %) shows the numerical increase or decrease relative to the baseline. * $p < 0.05$, ** $p < 0.01$, and *** $p < 0.001$. “/” means no significant change.

Delta waves in the frontal region significantly increased in HMD-VR compared to baseline ($p < 0.001$). Theta waves increased in the frontal region ($p < 0.05$), but decreased in the central ($p < 0.05$), parietal ($p < 0.01$), and occipital ($p < 0.01$) regions. Alpha waves decreased from baseline in the frontal ($p < 0.05$), central ($p < 0.001$), parietal ($p < 0.001$), occipital ($p < 0.001$), and temporal ($p < 0.001$) regions. Beta waves increased in the frontal region ($p < 0.001$), and decreased in the central ($p < 0.05$), parietal ($p < 0.001$), occipital ($p < 0.05$), and temporal ($p < 0.05$) regions. Gamma waves increased in the frontal region ($p < 0.001$), and decreased in the parietal region ($p < 0.05$). Table 2 presents significant differences in the absolute power of all frequency bands across all regions between baseline and HMD-VR. The topographical distribution of all frequency bands for baseline and HMD-VR is shown in Fig. 4.

HMD-VR	Frontal	Central	Parietal	Occipital	Temporal
Delta	Up *** (205%)	/	/	/	/
Theta	Up * (130%)	Down * (79%)	Down ** (71%)	Down ** (80%)	/
Alpha	Down * (62%)	Down *** (52%)	Down *** (39%)	Down *** (39%)	Down *** (5%)
Beta	UP *** (138%)	Down * (89%)	Down *** (73%)	Down * (82%)	Down * (90%)
Gamma	Up *** (159%)	/	Down * (81%)	/	/

Table 2. Significant changes in EEG frequency and area between baseline and induced cybersickness on a HMD ($n = 31$).

	Frontal				Central				Parietal				Occipital				Temporal			
	C	H	p	d	C	H	p	d	C	H	p	d	C	H	p	d	C	H	p	d
Delta	2.38 (4.54)	6.07 (9.73)	/	0.36	-0.7 (0.91)	0.32 (1.91)	/	0.18	-0.9 (1.80)	0.4 (3.56)	/	0.13	0.3 (2.57)	0.94 (5.31)	/	0.12	-0.07 (1.19)	1.92 (3.96)	/	0.48
Theta	0.37 (1.02)	0.74 (1.92)	/	0.18	-0.21 (0.66)	-0.39 (0.81)	/	0.21	-0.26 (0.66)	-0.68 (1.32)	/	0.17	-0.25 (0.92)	-0.56 (1.35)	/	0.18	-0.23 (0.49)	-0.23 (1.07)	/	0.16
Alpha	-1.31 (2.66)	-1.72 (3.6)	/	0.13	-1.33 (2.06)	-1.8 (2.57)	/	0.36	-2.73 (3.37)	-4.46 (5.55)	/	0.32	-3.54 (4.95)	-5.44 (7.03)	/	0.33	-0.42 (0.95)	-1.97 (2.7)	/	0.33
Beta	0.77 (1.14)	1.16 (2.0)	/	0.12	-0.1 (0.39)	-0.2 (0.5)	/	0.23	-0.32 (0.62)	-0.69 (1.06)	/	0.24	-0.25 (0.74)	-0.57 (1.18)	/	0.26	-0.09 (0.39)	-0.32 (0.79)	/	0.20
Gamma	0.91 (1.2)	1.52 (2.16)	/	0.48	0.11 (0.24)	0.02 (0.48)	/	0.00	-0.7 (0.38)	-0.3 (0.64)	/	0.54	-0.02 (0.53)	-0.22 (0.89)	/	0.26	-0.06 (0.45)	-0.1 (0.89)	/	0.04

Table 3. Average and paired t-test results for each waveform by region.

Here “Up” indicates significantly increased EEG frequencies compared to the baseline and “Down” means the opposite. The (n %) shows the numerical increase or decrease relative to the baseline. * $p < 0.05$, ** $p < 0.01$, and *** $p < 0.001$. “/” means no significant change.

When comparing curved-VR and HMD-VR, we observed that the common areas of response were the frontal region for delta waves, the frontal, central, parietal, occipital, and temporal regions for alpha waves, the frontal and parietal regions for beta waves, and the frontal region for gamma waves. These results indicate that delta and alpha frequencies are consistently associated with fluctuations in specific brain regions and frequency bands.

Comparison between curved-VR and HMD-VR

After conducting a series of paired-samples t-tests on the time-averaged change scores for each of the 25 band-region combinations, no significant differences were found between the two VR conditions in any of the 25 combinations (Table 3). This suggests that while both VR types induced changes from baseline, the pattern of these neurological changes was broadly similar between curved-VR and HMD-VR.

The supplementary ANCOVA results were consistent with the primary analysis. Although marginal p-values were observed in some regions, no variable reached statistical significance after applying the Bonferroni correction ($p < 0.002$), suggesting that the physiological response was comparable between the two display types.

C : curved-VR, H : HMD-VR () - Standard deviation, Cohen's d : effect size. A Bonferroni correction was applied to account for multiple comparisons ($\alpha = 0.05/25 = 0.002$). None of the p-values reached the corrected threshold for statistical significance.

Comparison of SSQ scores between curved-VR and HMD-VR and their correlation with EEG

SSQ scores in curved-VR and HMD-VR were observed to be higher in HMD for three subscores and the total score. However, the difference was only significant for the disorientation subscore, and no significant differences were found when comparing the subscores or the total scores between the two VR conditions (Fig. 5).

To investigate the relationship between EEG and SSQ, correlation analyses were performed. The results revealed no statistically significant correlations between any of the 25 EEG measures (5 waves \times 5 regions) and the SSQ scores (total Score, nausea, oculomotor, and disorientation) for either the curved-VR or the HMD-VR condition ($p < 0.05$).

Discussion

This study assessed subjective (SSQ) and objective (EEG) measures of cybersickness for two display types (HMD and curved monitor). We evaluated and compared the brain regions and frequency bands where EEG significantly deviated from baseline during cybersickness induced by the two display types. The analysis revealed that common frequencies and regions exhibiting significant EEG responses across the display types were found

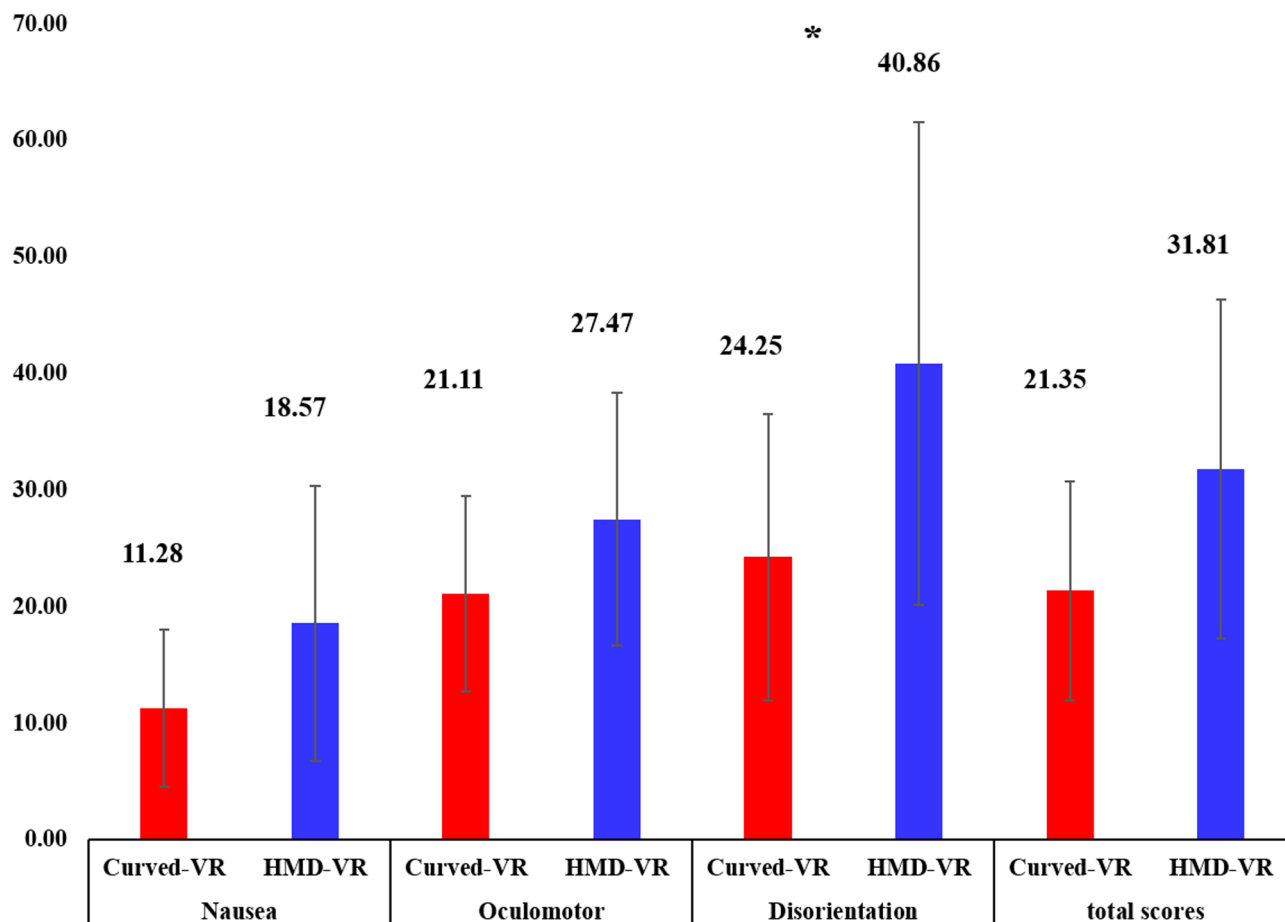


Fig. 5. SSQ score comparison for curved-VR and HMD-VR. Values above the bars represent the mean scores, with standard errors shown by the error bars. * $p < 0.05$.

in the delta and alpha bands. Direct comparisons of EEG spectral power between the Curved-VR and HMD-VR conditions did not reveal statistically significant differences. In order to better understand whether this lack of significance reflects a true similarity or was due to insufficient statistical power, we carefully examined both the effect sizes and the adequacy of our sample size. The analysis indicated generally small effect sizes (mostly Cohen's $d < 0.4$, see Table 3) for the EEG comparisons between displays. Moreover, considering that our sample size ($N = 31$) was quite close to the a priori requirement ($N = 34$) for detecting a medium effect size, we believe that the absence of a significant difference more likely reflects a genuine similarity in the visual processing load induced by both devices, rather than being solely due to limitations in sample size.

Cybersickness has been associated with consistent increases in delta wave activity across multiple studies^{32–34}. Given that delta waves are known to influence brain arousal, induce drowsiness, and play a role in the autonomic nervous system, and considering the frontal lobe's involvement in motor control and voluntary actions, EEG pattern changes are commonly observed in cybersickness contexts^{35,36}. In a VR task involving object finding with a rear-projection cave display system, increased delta power was reported as an indicator of cybersickness³². Similarly, a driving simulator equipped with a motion platform and a 360° rear-projection setup that provided both visual and vestibular input also revealed delta wave increases³³. In a test–retest study with individuals sensitive to cybersickness, elevated baseline delta activity was observed in the frontal lobe³⁴. Aligned with these findings, our study observed significant differences in delta wave activity across both display conditions. However, given the lack of correlation with subjective scores, we propose that these EEG responses likely serve as a physiological correlate of sensory conflict. This suggests that the observed neural patterns may reflect the brain's physiological response to the visual-vestibular mismatch, an aspect of cybersickness, independent of the individual's subjective report of distress. Notably, when examining the magnitude of percentage changes relative to baseline (Tables 1 and 2), the HMD-VR condition exhibited a more pronounced increase in Delta power (205% in the frontal region) compared to the Curved-VR condition (147%). Although the direct comparison between the two displays did not reach statistical significance after Bonferroni correction (Table 3), this trend indicates that the immersive HMD environment may induce larger relative physiological changes than the curved monitor.

Cybersickness-related EEG studies have shown mixed findings, with some reporting increased alpha power corresponding with more severe motion sickness symptoms during cybersickness induction^{16,33,37}, whereas others have observed a decrease in alpha activity among participants experiencing a virtual roller coaster on

a monitor screen³⁸. A reduction in alpha waves in the occipital and parietal channels was also found when participants were exposed to a first-person roller coaster simulation at three different speed conditions³⁹. This finding is consistent with the present study, and it is interpreted that the decrease in occipital and parietal alpha waves, which correspond to the visual cortex, is due to the participants' exposure to a visually unpleasant environment³⁹. Sensitive participants who watched a cybersickness-inducing video reported a significant decrease in alpha waves compared to baseline³⁴. A significant decrease in alpha wave activity was also observed in both sensitive and non-sensitive participants when they engaged with cybersickness-inducing VR content⁴⁰. To clarify whether this decline was due to cybersickness or merely visual stimulation, another study presented multiple types of visual stimuli and confirmed that the alpha reduction was attributable to cybersickness⁴¹. This decrease in alpha waves reflects changes in brain activity and indicates that the cognitive state is changing and becoming uncomfortable, which implies a focus on external stimuli^{42–44}. Our study using both types of displays showed the decrease in alpha waves. These results are consistent with previous studies that have reported a decrease in alpha waves as a sign of cybersickness.

EEG research on cybersickness has rarely focused on gamma wave activity. One study analyzed the EEG of participants who watched a VR content inducing cybersickness and found that gamma waves increased as the intensity of the motion sickness grew⁴⁵. Increased gamma waves were also observed in the EEG of participants who experienced cybersickness in a test-retest experiment³⁴. In a study that used aromatic scents to measure the reduction of cybersickness, the reduction was in the VR condition with aromatic scents compared to the VR condition without aromatic scents⁴⁶. Gamma waves are generally associated with sensory stimuli and are linked to various cognitive phenomena, including perceptual aggregation and higher-order information processing⁴⁵. Cybersickness is caused by sensory conflicts, and participants experience these conflicts in the brain, which may lead to an increase in gamma wave power as the brain attempts to resolve them⁴⁵. While an increase in gamma waves was observed in the frontal region for both display types, this wave was not consistent across the other measured regions. Therefore, additional research is required to determine the underlying causes of this region-specific increase in gamma wave activity.

EEG investigations of cybersickness have revealed mixed findings regarding beta wave activity, with some reporting increases and reporting decreases^{17,46,47}. This study, a decrease in beta wave activity was observed in the parietal region across both display types. The parietal lobe is located at the transitional zone between the somatosensory cortex and the motor cortex, and is involved in the integration of spatial representation that requires bodily sensory information derived from vestibular input³³. Therefore, this change may be associated with vestibular-based cybersickness. The beta and high-beta bands are associated with attention, cognition, and arousal, and decreased power in these bands can lead to a decreased sense of body position and cause dizziness or disorientation¹⁷. However, a decrease in beta waves was observed in the central, occipital, and temporal regions in the HMD condition, while no such significant changes were found for the curved monitor. Further research is needed to investigate these regional changes in beta waves under the influence of cybersickness.

Research on EEG responses to cybersickness has shown inconsistent findings regarding theta wave activity. Some studies have reported an increase in theta power with increasing motion sickness symptoms during cybersickness induction^{16,47}. A study in which participants were induced with cybersickness in 2D and 3D groups found a decrease in theta power in the frontal-temporal region in the 3D group¹⁷. The analysis of regional EEG showed no consistent findings between the two display types, with the changes observed in one condition not corresponding to the changes in the other.

In this study, correlation analyses showed no statistically significant relationship between any of the 25 EEG measures (5 EEG waves × 5 Brain regions) and the SSQ scores for either display type. Previous studies have reported a positive correlation between delta power and disorientation in the frontal area, and between delta power and oculomotor in the occipital area⁴⁰. A positive correlation was shown between alpha waves and questionnaire scores³³. A positive correlation between alpha and gamma power and motion sickness symptoms has also been observed in various brain areas, including motor, parietal, and occipital regions⁴⁸. Other studies have found a negative correlation between SSQ scores and alpha waves in the temporal region³⁴. In previous studies, a negative correlation between alpha2 (10–12 Hz) and SSQ's oculomotor and disorientation scores has been reported⁴⁹. Based on earlier findings, after the VR experience, absolute theta power showed a positive correlation, while absolute beta power showed a negative correlation⁵⁰. Given the contradictory statistical precedents (positive vs. negative), the absence of a clear linear correlation in our study may suggest a more complex relationship, rather than a straightforward one-to-one mapping. This is consistent with an increasing body of literature that indicates a possible dissociation between physiological signals and subjective symptom reporting^{25,51}. These studies highlight a key methodological distinction: while EEG captures the immediate, real-time neural effort involved in processing sensory conflicts during exposure, the SSQ reflects a retrospective and cumulative cognitive appraisal of symptoms, which is measured only after the experiment. This temporal mismatch may help explain why high physiological arousal during the task does not always translate directly into the subjective severity reported post-experiment. Building on this perspective to interpret the lack of EEG–SSQ correlation and the significant SSQ Disorientation difference, we propose that the observed Delta and Alpha changes reflect the physiological arousal and visual processing load required to resolve sensory conflicts. This interpretation aligns with our previous finding⁴¹, which demonstrated that Alpha reduction is not caused by simple visual stimulation (e.g., static images) but is specific to motion-induced cybersickness. Therefore, the EEG signals represent the brain's active effort to process the sensory conflict between visual motion and vestibular rest (Visual Load). In contrast, the significantly higher SSQ Disorientation scores observed in the HMD condition likely arise from the lack of a stationary reference frame, which exacerbates vestibular confusion. This aligns with previous findings linking disorientation symptoms to deficits in vestibular integration and cognitive spatial representation^{17,33}. It is important to acknowledge that HMD-specific hardware characteristics may have contributed to the observed SSQ Disorientation scores. Unlike the curved monitor, the HMD introduces

inherent technical confounders such as display latency (motion-to-photon lag) and the physical weight of the headset (approx. 770 g)^{2,31,52}. These factors could potentially induce vestibular-proprioceptive conflicts (due to latency) and physical fatigue (due to weight), both of which may influence disorientation and discomfort symptoms. Therefore, the significant difference in subjective reports may reflect the influence of these hardware-specific factors on the user experience, distinguishing it from the visual load captured by EEG. This distinction explains why the immediate neural response (EEG) does not linearly correlate with the subjective perception of disorientation (SSQ).

In our study, since a curved monitor was used to assess cybersickness, the relatively small difference in immersion compared to HMD may have contributed to the absence of significant EEG differences. The SSQ showed a tendency for higher scores in the HMD condition, with a significant difference observed in only one of the four scores. In contrast, no significant differences were observed in the EEG results. This suggests that, even with a sufficient number of channels used for EEG analysis (184 out of 256), the differences in EEG responses between HMD and curved monitor may be minimal. Therefore, EEG-based motion sickness experiments may not necessarily require the use of an HMD, as similar results might be expected with curved monitor or large displays that offer adequate levels of immersion.

There are some limitations to this study. First, the participants were a homogeneous group of men in their 20s with high Motion Sickness Susceptibility Questionnaire (MSSQ) scores. This demographic specificity limits the generalizability of our findings. Specifically, the observed lack of significant differences between display types may not hold for more diverse populations, such as women, older adults, or individuals with lower susceptibility. Therefore, future research expanding to these groups is necessary to validate whether the display-independent neural patterns persist across the general population. Second, this study excluded vertical elements from the content organization to reduce content complexity. We induced cybersickness in participants with HMD through content containing vertical elements to assess their brainwaves, which are currently being analyzed.

Conclusion

This study evaluated cybersickness using subjective (SSQ) and EEG-based physiological measures to compare responses across two display types. Consistent changes in delta and alpha activity were observed during cybersickness in both displays. These findings suggest that EEG responses associated with cybersickness may follow a similar pattern across display types, implying that the underlying neural mechanism may not be strongly dependent on the specific device used. However, given the demographic limitations of our sample, caution should be exercised in generalizing these results to broader populations.

Data availability

The data that support the findings of this study are available from the corresponding author upon reasonable request.

Received: 18 October 2025; Accepted: 12 December 2025

Published online: 31 January 2026

References

1. Kwon, C. Verification of the possibility and effectiveness of experiential learning using HMD-based immersive VR technologies. *Virtual Real.* **23**, 101–118 (2019).
2. Rebenitsch, L. & Owen, C. Review on cybersickness in applications and visual displays. *Virtual Real.* **20**, 101–125 (2016).
3. Lee, J., Kim, M., Kim, J. & RoleVR Multi-experience in immersive virtual reality between co-located HMD and non-HMD users. *Multimedia Tools Appl.* **79**, 979–1005 (2020).
4. Caserman, P., Garcia-Agundez, A., Gámez Zerban, A. & Göbel, S. Cybersickness in current-generation virtual reality head-mounted displays: systematic review and outlook. *Virtual Real.* **25**, 1153–1170 (2021).
5. Porcino, T., Trevisan, D. & Clua, E. A cybersickness review: causes, strategies, and classification methods. *J. Interact. Syst.* **12**, 269–282 (2021).
6. Biswas, N., Mukherjee, A. & Bhattacharya, S. Are you feeling sick?—A systematic literature review of cybersickness in virtual reality. *ACM Comput. Surveys.* **56**, 1–38 (2024).
7. Reason, J. T. & Brand, J. J. *Motion Sickness* (Academic, 1975).
8. Keshavarz, B., Riecke, B. E., Hettlinger, L. J. & Campos, J. L. Vection and visually induced motion sickness: how are they related? *Front. Psychol.* **6**, 472 (2015).
9. Chang, E., Kim, H. T. & Yoo, B. Virtual reality sickness: a review of causes and measurements. *Int. J. Human-Computer Interact.* **36**, 1658–1682 (2020).
10. Kennedy, R. S., Lane, N. E., Berbaum, K. S. & Lilienthal, M. G. Simulator sickness questionnaire: an enhanced method for quantifying simulator sickness. *Int. J. Aviat. Psychol.* **3**, 203–220 (1993).
11. Rebenitsch, L. & Owen, C. in *Proceedings of the 27th annual ACM symposium on User interface software and technology*. 309–317.
12. Fernandes, A. S. & Feiner, S. K. in *2016 IEEE symposium on 3D user interfaces (3DUI)*. 201–210 (IEEE).
13. Garcia-Agundez, A., Reuter, C., Caserman, P., Konrad, R. & Göbel, S. Identifying cybersickness through heart rate variability alterations. *Int. J. Virtual Real.* **19**, 1–10 (2019).
14. JESSICA, B. B. Systematic investigation of physiological correlates of motion sickness induced by viewing an optokinetic rotating drum. *Aviat. Space Environ. Med.* **70**, 759–765 (1999).
15. Guna, J. et al. Influence of video content type on users' virtual reality sickness perception and physiological response. *Future Generation Comput. Syst.* **91**, 263–276 (2019).
16. Krokos, E. & Varshney, A. Quantifying VR cybersickness using EEG. *Virtual Real.* **26**, 77–89 (2022).
17. Naqvi, S. A. A. et al. EEG based time and frequency dynamics analysis of visually induced motion sickness (VIMS). *Australasian Phys. Eng. Sci. Med.* **38**, 721–729 (2015).
18. Park, M. C. & Mun, S. Overview of measurement methods for factors affecting the human visual system in 3D displays. *J. Disp. Technol.* **11**, 877–888 (2015).
19. Chang, E., Seo, D., Kim, H. T. & Yoo, B. An integrated model of cybersickness: Understanding user's discomfort in virtual reality. *J. KIISE.* **45**, 251–279 (2018).

20. Chang, E., Billinghurst, M. & Yoo, B. Brain activity during cybersickness: a scoping review. *Virtual Real.* **27**, 2073–2097 (2023).
21. Hakkinen, J., Vuori, T. & Paakka, M. in *IEEE international conference on systems, man and cybernetics*. 147–152 (IEEE Yasmine Hammamet).
22. Sharples, S., Cobb, S., Moody, A. & Wilson, J. R. Virtual reality induced symptoms and effects (VRISE): comparison of head mounted display (HMD), desktop and projection display systems. *Displays* **29**, 58–69 (2008).
23. Liu, C. L. & Uang, S. T. in *Human-Computer Interaction. Users and Applications: 14th International Conference, HCI International Orlando, FL, USA, July 9–14, 2011, Proceedings, Part IV* 14. 490–499 (Springer). (2011).
24. Kim, K., Rosenthal, M. Z., Zielinski, D. J. & Brady, R. Effects of virtual environment platforms on emotional responses. *Comput. Methods Programs Biomed.* **113**, 882–893 (2014).
25. Dennison, M. S., Wisti, A. Z. & D’Zmura, M. Use of physiological signals to predict cybersickness. *Displays* **44**, 42–52 (2016).
26. Keshavarz, B., Hecht, H. & Zschuschke, L. Intra-visual conflict in visually induced motion sickness. *Displays* **32**, 181–188 (2011).
27. Urakami, J. et al. Comparing immersiveness and perceptibility of spherical and curved displays. *Appl. Ergon.* **90**, 103271 (2021).
28. Mun, S., Park, M. C. & Yano, S. Evaluation of viewing experiences induced by a curved three-dimensional display. *Opt. Eng.* **54**, 103104–103104 (2015).
29. Stanney, K., Fidopiastis, C. & Foster, L. Virtual reality is sexist: but it does not have to be. *Front. Rob. AI.* **7**, 4 (2020).
30. Clemes, S. A. & Howarth, P. A. The menstrual cycle and susceptibility to virtual simulation sickness. *J. Biol. Rhythm.* **20**, 71–82 (2005).
31. Davis, S., Nesbitt, K. & Nalivaiko, E. in *Proceedings of the 2014 conference on interactive entertainment*. 1–9.
32. Kim, Y. Y., Kim, H. J., Kim, E. N., Ko, H. D. & Kim, H. T. Characteristic changes in the physiological components of cybersickness. *Psychophysiology* **42**, 616–625 (2005).
33. Chen, Y. C. et al. Spatial and Temporal EEG dynamics of motion sickness. *NeuroImage* **49**, 2862–2870 (2010).
34. Lim, H. K. et al. Test-retest reliability of the virtual reality sickness evaluation using electroencephalography (EEG). *Neurosci. Lett.* **743**, 135589 (2021).
35. Knyazev, G. G. EEG delta oscillations as a correlate of basic homeostatic and motivational processes. *Neurosci. Biobehavioral Reviews*. **36**, 677–695 (2012).
36. Güntekin, B. & Başar, E. Review of evoked and event-related delta responses in the human brain. *Int. J. Psychophysiol.* **103**, 43–52 (2016).
37. Kim, J., Kim, W., Oh, H., Lee, S. & Lee, S. in *Proceedings of the IEEE/CVF international conference on computer vision*. 10580–10589.
38. Baumgartner, T., Valko, L., Esslen, M. & Jäncke, L. Neural correlate of Spatial presence in an arousing and noninteractive virtual reality: an EEG and psychophysiology study. *CyberPsychology Behav.* **9**, 30–45 (2006).
39. Celikkan, U. in *2019 3rd international symposium on multidisciplinary studies and innovative technologies (ISMSIT)*. 1–4 (IEEE).
40. Jang, K. M., Kwon, M., Nam, S. G., Kim, D. & Lim, H. K. Estimating objective (EEG) and subjective (SSQ) cybersickness in people with susceptibility to motion sickness. *Appl. Ergon.* **102**, 103731 (2022).
41. Lee, D. H., Jang, K. M. & Lim, H. K. Electroencephalography changes during cybersickness: focusing on delta and alpha waves. *Brain Topogr.* **38**, 1–10 (2025).
42. Mo, J., Liu, Y., Huang, H. & Ding, M. Coupling between visual alpha oscillations and default mode activity. *Neuroimage* **68**, 112–118 (2013).
43. Sadaghiani, S. & Kleinschmidt, A. Brain networks and α -oscillations: structural and functional foundations of cognitive control. *Trends Cogn. Sci.* **20**, 805–817 (2016).
44. Naqvi, S. A. A., Badruddin, N., Malik, A. S., Hazabbah, W. & Abdullah, B. in *5th international conference on intelligent and advanced systems (ICIAS)*. 1–5 (IEEE). 1–5 (IEEE). (2014).
45. Lin, Y. T., Chien, Y. Y., Wang, H. H., Lin, F. C. & Huang, Y. P. in *SID Symposium Digest of Technical Papers*. 862–865 (Wiley Online Library).
46. Oh, S. H. & Whangbo, T. K. in *2018 International conference on information and communication technology convergence (ICTC)*. 568–570 (IEEE).
47. Chang, E. et al. in *2013 International winter workshop on brain-computer interface (BCI)*. 62–64 (IEEE).
48. Chuang, S. W., Chuang, C. H., Yu, Y. H., King, J. T. & Lin C.-T. EEG alpha and gamma modulators mediate motion sickness-related spectral responses. *Int. J. Neural Syst.* **26**, 1650007 (2016).
49. Kim, J. Y., Son, J. B., Leem, H. S. & Lee, S. H. Psychophysiological alteration after virtual reality experiences using smartphone-assisted head Mount displays: an EEG-based source localization study. *Appl. Sci.* **9**, 2501 (2019).
50. Heo, J. & Yoon, G. EEG studies on physical discomforts induced by virtual reality gaming. *J. Electr. Eng. Technol.* **15**, 1323–1329 (2020).
51. Gavvani, A. M., Nesbitt, K. V., Blackmore, K. L. & Nalivaiko, E. Profiling subjective symptoms and autonomic changes associated with cybersickness. *Auton. Neurosci.* **203**, 41–50 (2017).
52. Souchet, A. D., Lourdeaux, D., Pagani, A. & Rebenitsch, L. A narrative review of immersive virtual reality’s ergonomics and risks at the workplace: cybersickness, visual fatigue, muscular fatigue, acute stress, and mental overload. *Virtual Real.* **27**, 19–50 (2023).

Author contributions

Authors: Dong-Hyun Lee(A), MS, Kyoung-Mi Jang (B), PhD, Hyun Kyoon Lim (C), PhD(C) and (B) designed the research. (A) and (B) performed the experiments. (A) analyzed the data. (C) and (A) wrote the main manuscript text. All authors reviewed the manuscript.

Funding

This work was supported by the Ministry of Trade, Industry, and Energy (MOTIE), Korea, under the “Regional industry-based organization support program” [grant number: P0001940] supervised by the Korea Institute for Advancement of Technology (KIAT).

Declarations

Competing interests

The authors declare no competing interests.

Additional information

Correspondence and requests for materials should be addressed to H.K.L.

Reprints and permissions information is available at www.nature.com/reprints.

Publisher's note Springer Nature remains neutral with regard to jurisdictional claims in published maps and institutional affiliations.

Open Access This article is licensed under a Creative Commons Attribution-NonCommercial-NoDerivatives 4.0 International License, which permits any non-commercial use, sharing, distribution and reproduction in any medium or format, as long as you give appropriate credit to the original author(s) and the source, provide a link to the Creative Commons licence, and indicate if you modified the licensed material. You do not have permission under this licence to share adapted material derived from this article or parts of it. The images or other third party material in this article are included in the article's Creative Commons licence, unless indicated otherwise in a credit line to the material. If material is not included in the article's Creative Commons licence and your intended use is not permitted by statutory regulation or exceeds the permitted use, you will need to obtain permission directly from the copyright holder. To view a copy of this licence, visit <http://creativecommons.org/licenses/by-nc-nd/4.0/>.

© The Author(s) 2026